ANALYTICAL AND NUMERICAL APPROACH FOR LOAD CAPACITY OF A SINGLE SQUARE CELL FROM A TEXTURED SURFACE

V. MARIAN, M. PASCOVICI, Tr. CICONE*

Texturarea suprafeţelor lubrifiate contribuie la reducerea coeficientului de frecare şi a ratei de uzare a suprafeţelor. Lucrarea de faţă prezintă un studiu analitic şi numeric al forţei portante şi al coeficientului de frecare în cazul unei degajări de formă pătrată, degajare realizată de regulă prin procedeul fotolitografic. Modelul analitic este bazat pe liniarizarea distribuţiei de presiuni iar modelul numeric se bazează pe utilizarea metodei diferenţelor finite. Este prezentată de asemenea o comparaţie a rezultatelor obţinute prin cele două metode. Se constată o bună corelaţie între rezultatele obţinute prin metoda analitică şi cele obţinute prin metoda numerică.

Lubricated textured surfaces reduce the friction coefficient and the surface wear rate. The present work is dedicated to the analytical and numerical study of load capacity and friction coefficient of a single, square dimple, typical for textured surfaces realized by lithography. The analytical model is based on the pressure linearization while the numerical model on the finite difference method. A comparison between the results obtained by the two methods is presented. It is shown that the results obtained by the analytical method are close to the results obtained by the numerical method.

Keywords: Hydrodynamic Lubrication, Textured Surfaces, Parallel Slider, Finite Difference Method

Introduction

The important role played by roughness in fluid film applications has been recognized since the beginning of modern studies in lubrication. However, only in the last decade, controlled roughness was systematically analyzed as a possible mechanism for lift-off effects, for nominally parallel sliding surfaces. This evolution reflected by the great number of recent papers (see Fig. 10 (created by the authors)) is correlated with the recent developments of new and improved techniques for creating surfaces with controlled microstructure or patterns. Indentation, chemical etching, micromachining, laser ablation, LIGA processes,

* PhD. Student, Prof., Reader, Dept. of Machine Elements and Tribology, University POLITEHNICA of Bucharest, Romania

etc., have recently become available for large scale production of textured surfaces. These techniques for "surface texturing" allow creation of well defined "dimples" regularly distributed on the surface.

It is generally accepted that surface texturing can be benefic for lubricated pairs in several ways: increased capacity, reduced friction, increased film stiffness or providing a lubricant storage [2], [6]. On a micro-scale, dimples on textured surfaces have the same effects as the pocket in step bearings [15] or an inclined pad [5].

The geometry of a dimple can take various configurations, function of the technique used for texturing. Cylindrical, conical, spherical or parallelepiped configurations are typical models for real dimples.

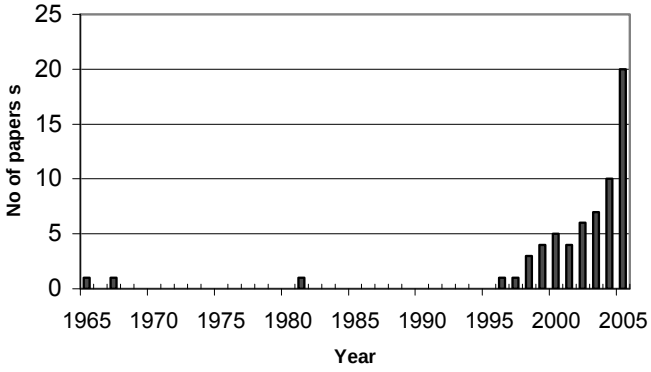

Fig. 1 Number of published papers related to surface texturing

A review of the present state-of-the art for textured surfaces modeling show that few papers present numerical solutions for pressure generation in the case of square dimples and an analytical solution has not been yet developed.

Wang et al. [14] presents the first analytical approach based on standard Rayleigh step bearing model. However, the use of the equations for an infinite pad is questionable. They conclude that for cylindrical dimples there exists a theoretical optimum of 40% in the dimple area ratio.

Brizmer and co-workers present in a series of papers a numerical solution for Reynolds equation for spherical dimples, obtained by laser techniques [6].

Siripuram et al. [12] and Burstein et al. [7] present the effect of different dimple geometry (including the square dimples) on the load carrying capacity of mechanical seals.

The present work is dedicated to the study of load capacity of a single, square dimple typical for textured surfaces realized by lithography [1] [10]. This procedure allows a better control of the depth of each dimple in respect with classical laser-textured technique.

The analysis is performed using two models: a simple analytical model and a more complex, 2D numerical model. Reported to the literature presented above the original part of the article is the analytical solution who offers a fast and reliable method for determining the load capacity and the friction coefficient. The results predicted with each of the models are compared and conclusions on optimum design parameters are obtained.

Nomenclature

F – load capacity
F_f – friction force
$\bar{F}$ – dimensionless load, $\frac{Fh_m^2}{\eta UL^3}$
$\bar{F}_f$ - dimensionless friction force, $\frac{F_f h_m}{\eta UL^2}$
h – film thickness
$\bar{h}$ – dimensionless film thickness, h/h_m
h_m – minimal film thickness (film thickness on the lands)
ℓ – dimple characteristic dimension
L – cell characteristic dimension
p – pressure
p_{max} – maximum pressure
$\bar{p}$ – dimensionless pressure, $\frac{ph_m^2}{\eta UL}$
$\bar{p}_{\max}$ – maximum dimensionless pressure
Q – rate of flow
s – dimple depth
$\bar{s}$ - dimensionless dimple depth, s/h_m
U – sliding velocity
x – longitudinal Cartesian coordinate
y – lateral Cartesian coordinate
$\bar{x}$ – dimensionless longitudinal coordinate, x/L
$\bar{y}$ – dimensionless lateral coordinate, y/L
η – dynamic viscosity
Δ – discretization step
ρ_t – dimple area density, ℓ^2/L^2
μ- friction coefficient
$\bar{\mu}$ - "dimensionless" friction coefficient, $\frac{\bar{F}_f}{\bar{F}}$

1. General assumptions

A uniform textured surface is considered so that a single dimple can be isolated with the associated neighboring lands, forming a square cell, of

characteristic length, L. Neglecting the interactions between dimples, the analysis can be restricted at a single dimple. The dimple surface is assumed square and its depth s, uniform, (Fig. 2). The area covered by the dimple reported to the area of the cell defines the dimple area density, ρ_t. The mating surface is assumed plane, perfectly smooth and parallel to the textured surface.

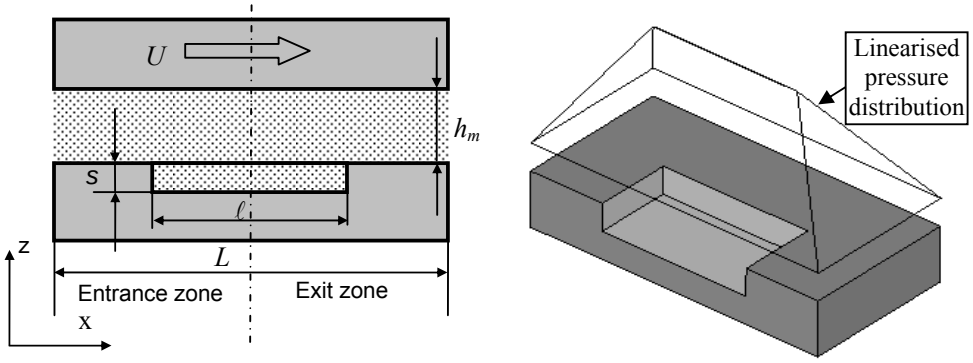

Fig. 2 Pressure distribution for the analytical model

The present analysis is based on the typical assumptions of fluid film lubrication, as follows:

(1) The fluid is Newtonian, incompressible, in laminar and isothermal flow, without slip at solid boundaries;

(2) Constant pressure across the film thickness;

(3) Neglected inertia effects;

(4) Zero pressure at the boundaries of the cell.

2. Analytical model

A simple analytical model to calculate hydrodynamic pressure generated by a single dimple can be obtained using a simplified pressure distribution.

Each dimple is assumed to be antisymmetric, that is, the pressure is negative in the entrance zone and positive in the exit zone (Fig. 3). Assuming a cavitation pressure equal to zero, the pressure on the entrance zone does not generate load capacity and consequently the leading half of the dimple can be considered as a classical Rayleigh pocket-step bearing. A linear pressure distribution can be assumed on both longitudinal and lateral directions (Fig. 2). Consequently, the load capacity can be written in terms of maximum pressure, generated at step border:

$$F = p_{\max}\frac{L}{2}\ell + \frac{2}{3}p_{\max}\frac{L-\ell}{2}\frac{L}{2} \tag{1}$$

The maximum pressure yields equating the flow rate in the dimple with the flow rate on the land. After some algebra calculi there results:

$$p_{\max} = \frac{3\eta U s \ell}{(h_m + s)^3 + \left(\frac{L-\ell}{\ell} + \frac{2\cdot L}{L-\ell}\right)h_m{}^3} \tag{2}$$

In dimensionless form, the maximum pressure is

$$\overline{p}_{\max} = \frac{3\sqrt{\rho_t}\ \overline{s}}{(\overline{s}+1)^3 + \left(\frac{1-\sqrt{\rho_t}}{\sqrt{\rho_t}} + \frac{2}{1-\sqrt{\rho_t}}\right)} \tag{3}$$

By substituting Eq. (2) in (1) one can obtain the load capacity:

$$F = L^2\frac{p_{\max}}{6}\left(1+\frac{\ell}{2L}\right) \tag{4}$$

or in dimensionless form:

$$\overline{F} = \frac{\overline{p}_{\max}}{6}\left(1+\frac{\sqrt{\rho_t}}{2}\right) \tag{5}$$

In Fig. 3 the load capacity is plotted as function of two geometric dimensionless parameters: $\overline{s}$ and ρ_t.

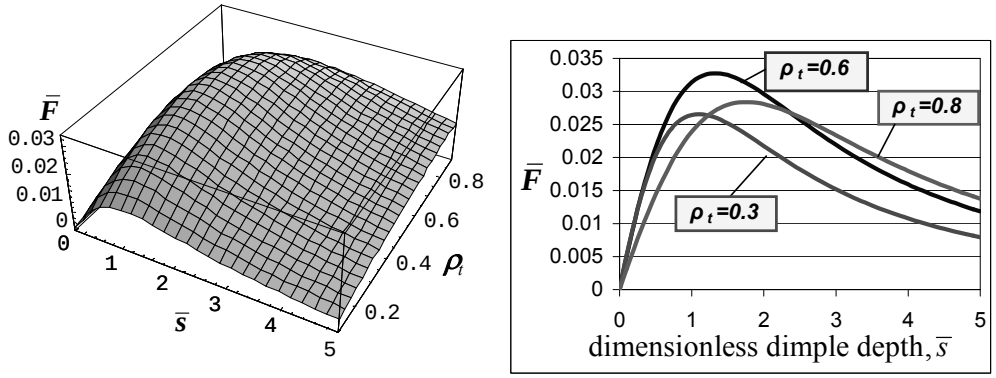

Fig. 3 Dimensionless force distribution

From Fig. 3 one can see that the load capacity has a maximum which can be easily obtained by solving, for $\bar{s}$ and ρ_t, the system of equations:

$$\frac{\partial}{\partial \rho_t}\bar{F} = 0 \tag{6}$$

$$\frac{\partial}{\partial \bar{s}}\bar{F} = 0 \tag{7}$$

Using a simple numerical procedure there results ρ_t*=0.6, $\bar{s}$*=1.33 and correspondingly, the maximum dimensionless load $\bar{F}_{\max}$ = 0.033.

Considering that there is no friction in the negative pressure zone, the friction force is:

$$\left|F_f\right| = \frac{\eta U(L^2-\ell^2)}{2h_m} + \frac{\eta U \ell^2}{2(h_m+s)} + \frac{p_{\max}\ell s}{2} \tag{8}$$

or in dimensionless coordinates:

$$\left|\bar{F}_f\right| = \frac{\left|F_f\right| h_m}{\eta U L^2} = \frac{1}{2} - \frac{\rho_t \bar{s}}{2(1+\bar{s})} + \frac{\bar{p}_{\max}}{2}\bar{s}\sqrt{\rho_t} \tag{9}$$

The "dimensionless" friction coefficient is:

$$\bar{\mu} = \frac{\bar{F}_f}{\bar{F}} = \frac{\mu L}{h_m} \tag{10}$$

The distribution of the friction coefficient function of the main parameters of the cell is presented in Fig. 4.

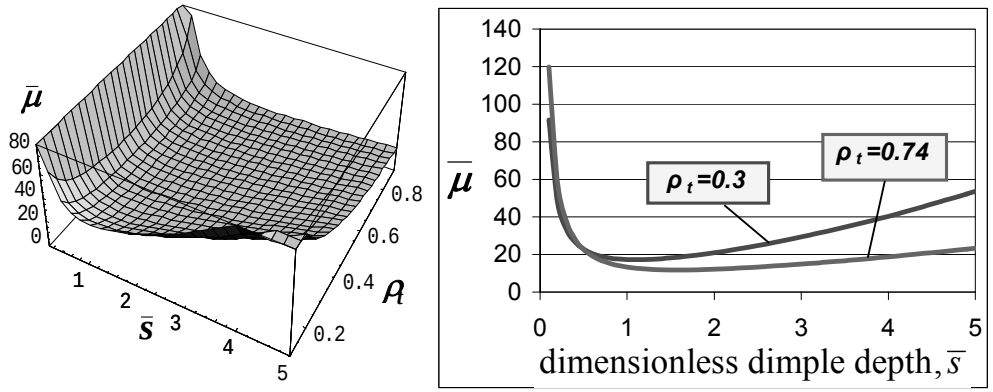

Fig. 4 Dimensionless friction coefficient distribution

From Fig. 4 one can see that the friction has a minimum which can be easily obtained solving, for $\bar{s}$ and ρ_t, the system of equations:

$$\frac{\partial}{\partial \rho_t}\bar{\mu} = 0 \tag{11}$$

$$\frac{\partial}{\partial \bar{s}}\bar{\mu} = 0 \tag{12}$$

Using also a simple numerical procedure there results ρ_t*=0.74, $\bar{s}^*$=1.58 and correspondingly, the dimensionless friction coefficient $\bar{\mu}_{\min}$ = 11.75.

3. Numerical Model

A more accurate analysis of performance characteristics of a single cell with a square dimple can be done solving numerically the Reynolds equation on each part of the cell and using a flow rate conservation law at the borders of the dimple. As the surfaces are nominally parallel, the Reynolds equation takes the simple form of Laplace Equation

$$\frac{\partial^2 p}{\partial x^2} + \frac{\partial^2 p}{\partial y^2} = 0 \tag{13}$$

As for the analytical model the boundary conditions are zero pressure on each limit of a cell. A classical finite differences scheme is used. The equations of fluid flow are:

$$Qx_{i,j,k} = \frac{1}{2}\left(\frac{1}{2}U\Delta h_{i,j} + \frac{h_{i,j}{}^3(p_{i+k,j} - p_{i+k,1+j})}{12\eta}\right) \tag{14}$$

$$Qy_{i,j,k} = \frac{1}{2}\left(\frac{h_{i,j}{}^3(p_{i,j+k} - p_{i+1,j+k})}{12\eta}\right) \tag{15}$$

where $Qx_{i,j,k}$ is the flow on a half of the finite volume side in x direction (k=0-upper side, k=1-lower side), $Qy_{i,j,k}$ is the flow on a half of the finite volume side in y direction (k=0-left, k=1-right side), $h_{i,j}$ is the fluid film thickness of a finite volume having the nodes coordinate (i,j), (i,j+1), (i+1,j+1), (i+1,j).

The Laplace equation on the parallel surfaces is:

$$p_{i,j} = \frac{1}{4}(p_{i-1,j} + p_{i,j-1} + p_{i,j+1} + p_{i+1,j}) \tag{16}$$

For the discontinuity points the flow conservation is used (Fig. 5).

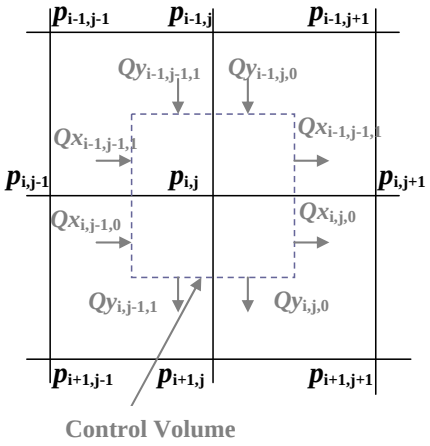

Fig. 5 Finite difference model

The shear tension on a grid element is:

$$\bar{\tau}_{i,j} = \frac{\tau_{i,j} h_m}{\eta U} = -\frac{1}{\bar{h}_{i,j}} - \frac{N\bar{h}_{i,j}}{2}(\bar{p}_{i,j+1} - \bar{p}_{i,j} + \bar{p}_{i+1,j+1} - \bar{p}_{i+1,j}) \qquad (17)$$

The dimensionless friction force becomes:

$$\bar{F}_f = \frac{F_f h_m}{\eta U L^2} = \int_0^1 \int_0^1 \bar{\tau}\, d\bar{x} d\bar{y} \qquad (18)$$

A Gauss-Seidel algorithm with over-relaxation has been implemented in a FORTRAN code.

4. Results and discussion

A first step of the numerical analysis was dedicated to the study of the convergence and consistency of the finite differences scheme. A standard procedure consisting of performing the numerical analysis on several successively finer grids has been used to define the discretization error. Five successive grids have been used and the error has been defined in terms of load capacity:

$$\varepsilon = 100 \cdot \frac{\bar{F} - \bar{F}_{exact}}{\bar{F}_{exact}}$$

where the "exact" solution was considered the value corresponding to the finest grid. A typical result is plotted in Fig. 6.

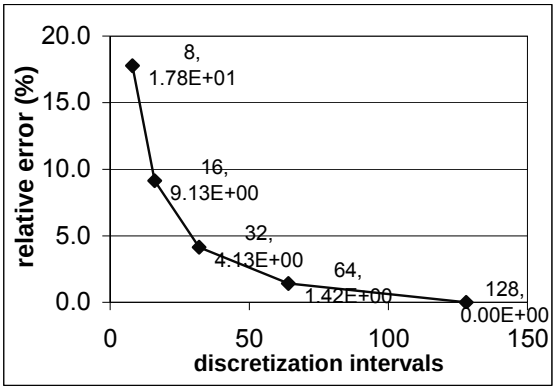

Fig. 6 Relative error evolution function of grid density

It is shown that the solution presents an asymptotic convergence to a "theoretical" value. The number of nodes chosen for the further simulations is 64, producing a relative error of 1.45%.

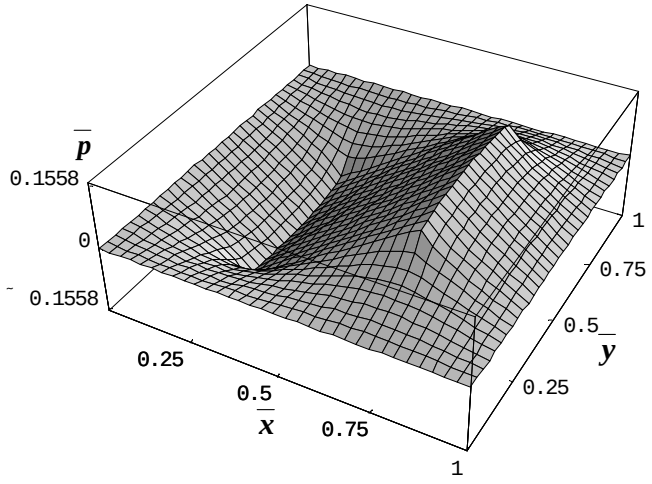

Fig. 7 Dimensionless pressure distribution on a square cell

In Fig. 7 the dimensionless pressure distribution is presented on a square dimple with the following characteristics: $\bar{s}=1$, $\rho_t=0.25$. In the zones where the pressure distribution is negative, the cavitation phenomenon appears. Therefore, in the calculation of the load carrying capacity only the positive values of the pressure distribution are considered.

A comparison between the results obtained by the analytical and numerical method is considered in Fig. 8 and Fig. 9 by varying the texture density and the dimensionless depth of the dimple. In both cases only the positive pressures are considered to contribute to the load carrying capacity. The variation intervals of the two parameters were chosen to cover the cases encountered in practice. The values of the fixed parameters are the optimal values obtained for the analytical solution ($\bar{s}=1.33$ and $\rho_t=0.6$ for load capacity and $\bar{s}=1.58$ and $\rho_t=0.74$ for friction coefficient).

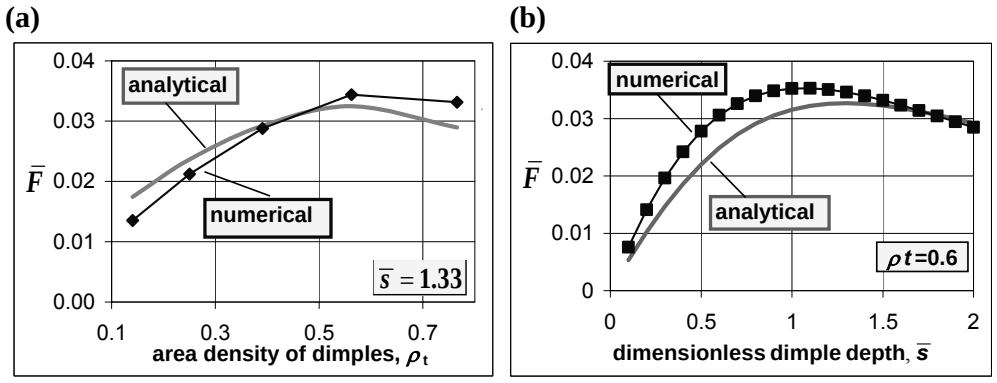

Fig. 8 Load capacity distribution function of cell parameters

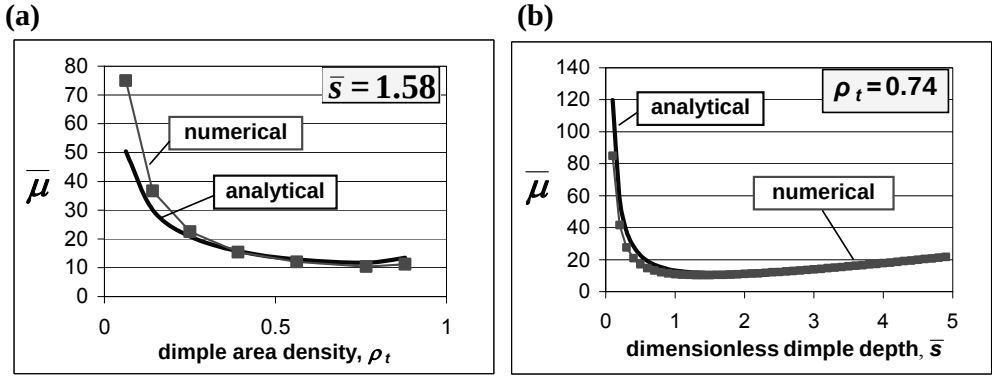

Fig. 9 Friction coefficient distribution function of cell parameters

It can be observed that there is a good correlation between the values of the analytical solution and the values of the numerical one. However, the analytical solution can be used to provide an approximate value of the load capacity while the numerical solution can be utilized to obtain a closer value of the real load capacity.

For a dimensionless dimple depth of 1.33, the analytical and numerical curves present a maximum dimensionless load for ρ_t=0.56 (Fig. 8, (a)). For a constant ρ_t=0.56, the analytical curve presents a maximum at $\bar{s}$=1.3 while the numerical solution at $\bar{s}$=1.1 (Fig. 8 (b)).

Both numerical and analytical solutions present the same optimal values to achieve a minimal friction coefficient (ρ_t=0.74, $\bar{s}$=1.58).

It can also be remarked that the optimal values in terms of load capacity are not the same as the optimal values of friction coefficient.

Conclusions

The theoretical modeling of a textured cell represents the first step in understanding the phenomena involved in the lubrication of textured surfaces, creating the premises of modeling a textured surface pair. The present paper analyses the load capacity and friction loss for a single, square dimple, using two models: a simplified analytical one and a more complex numerical model. Parametric analyses have revealed optimal load capacity and friction coefficient function for two important dimple parameters: area density and dimple depth. It is found that the textured density which maximizes the load carrying capacity of the cell is 0.6 while the dimensionless height of the dimple is 1.33. The parameters which minimize the friction coefficient are $\bar{s}^*$=1.58 and ρ_t*=0.74.

Comparisons between predicted analytical and numerical performance characteristics have shown good correlation, with differences within 10%.

Aknoledgments

Financial support for the work described in this paper was provided by National Council for Academic Scientific Research (CNCSIS) under Grants No. 1418/2004 and 464/2004.

R E F E R E N C E S

1. *Alberdi, A. , Merino, S., Barriga, J., Arazabe, A.*, Microstructured surfaces for tribological applications, 14th International Colloquium Tribology, Esslingen, pp.269-278, 2004

2. *Abeln, T., Klink, U*., Laserstrukturierung-Verbesserung der tribologischen Eigenschaften von Oberflachen, 14th International Colloquium Tribology, Esslingen, Germany, Vol.1, pp.315-319, 2004
3. *Anno, J.N., Walowit, J.A., Allen, C.M.*, Microasperity lubrication, ASME Annual Meeting, November 12-17, Paper No. 67-WA/Lub-1, 1967
4. *Arghir, M., Roucou, N., Helene, M., and Frene, I.*, Theoretical analysis of the incompressible laminar flow in a macro-roughness cell, ASME Journal of Tribology, 125(2), pp. 309-318, April 2003
5. *Brajdnic-Mitidieri ,P., Gosman, A. D., Ioannindes, E., Spikes, H.*, CFD Analysis of a low friction pocketed pad bearing, Journal of Tribology, Vol.127, pp.803-812, 2006
6. *Brizmer V, Klingerman, Y, Etsion, I.*, A laser surface textured parallel thrust bearing, Tribology Transactions, Vol 46, No 3, pp. 397-403, 2003
7. *Burstein, L., Ingman, D.,* Effect of pore ensemble statistics on load support of mechanical seals with pore-covered faces, Journal of Tribology, Vol.121, pp.927-932, 1999
8. *Dobrică M., Fillon M.*, Thermohydrodynamic Behaviour of a Slider Pocket Bearing, Journal of Tribology, Vol. 128., pp. 312-318, 2006
9. *Hamilton, D.B., Walowit, J.A., Allen, C.M.*, A Theory of Lubrication by Micro-irregularities, ASME-ASLE Lubrication Conference, October 18-20 Paper No. 65-Lub-11, 1965
10. *Pettersson, U., Jacobson, S.*, Influence of surface texture on boundary lubricated sliding contacts, Tribology International, Vol 36, pp. 857-864, 2003
11. *Sahlin, F., Glavatskih, S., Torbjörn, A., Larsson, R.*, Two-Dimensional CFD-Analysis of Micro-Patterned Surfaces in Hydrodynamic Lubrication, Journal of Tribology, Vol. 127, pp. 96-102
12. *Siripuram, R., Stephens, L.*, Efect of deterministic asperity geometry on hydrodynamic lubrication, Proceedings of 2003 STLE/ASME Joint Tribology Conference, October 26-29, 2003
13. *Tonder, K.*, A new class of bearings based on roughness effects, STLE/ASME Tribology Conference, Orlando, 1999
14. *Wang, X., Kato, K., Adachi, K., Aizawa, K.*, Loads carrying capacity map for the surface texture design of SiC thrust bearing sliding in water, Tribology International, Vol. 36, pp. 189-197, 2003
15. *Wilcock D. F., Schenectady N.Z.*, The Hydrodynamic Pocket Bearing, Transactions of the ASME, April, 1955